

# MODEL FOR INTERLAYER SPACING OF MULTIWALL CARBON NANOTUBES

X. Sun<sup>a</sup>, H. J. Zeiger<sup>a</sup>, C.-H. Kiang<sup>a,b</sup>, M. S. Dresselhaus<sup>a,c</sup>, M. Endo<sup>d</sup>

<sup>a</sup>Department of Physics, Massachusetts Institute of Technology, Cambridge, Massachusetts 02139

<sup>b</sup>Present address: Department of Chemistry and Biochemistry, University of California, Los Angeles, CA 90024

<sup>c</sup>Department of Electrical Engineering and Computer Science, Massachusetts Institute of Technology,  
Cambridge, Massachusetts 02139

<sup>d</sup>Department of Electrical and Electronic Engineering, Faculty of Engineering, Shinshu University, Nagano 380,  
Japan

The discovery of carbon nanotubes<sup>1</sup> has prompted numerous studies of the structure, properties and potential applications of these exotic materials. Currently, most of the anticipated properties and applications are based on theoretical calculations for idealized nanotube structures.<sup>2-5</sup> A precise knowledge of the structure of real nanotubes is essential for an accurate evaluation of the potential applications. In the present work, we study the high resolution transmission electron microscope (HRTEM) tube images for several different multi-layer carbon nanotubes in an effort to understand the previously-reported variation in the inter-shell spacing.<sup>1,6-9</sup> To obtain quantitative results, we carried out a digital image analysis of high resolution TEM images, which allows us to relate the inter-shell spacings to the nanotube diameter.

Carbon nanotube samples were prepared by the usual arc-discharge method<sup>1,10</sup>. The core of the deposit was crushed and dispersed in ethanol. A drop of this solution was transferred to a holey carbon microscope grid for TEM examination. High resolution TEM images were obtained in a TOPCON 002B microscope at 200KV or a JEOL 4000 EX at 400KV accelerating voltage. The images were scanned with a CCD camera, and the captured images were stored in a  $1024 \times 1024$  pixel array of 256 gray-scale levels.

We carried out high resolution image analysis of nanotubes in real space, which allowed us to measure individual inter-shell spacings as a function of tube diameter.<sup>11</sup> Each data point is obtained as an average over 5 measurements to reduce the error, as shown in Fig. 1. Our data for all tube diameters that were studied show that the inter-shell spacing ( $\hat{d}_{002}$ ) ranges from 0.33 to 0.39 nm, and that  $\hat{d}_{002}$  increases as the tube diameter decreases.

Figure 2 shows the experimental data of inter-shell spacing as a function of tubule diameter for three different nanotubes. A simple theoretical model is proposed to explain the increase of inter-shell spacing with decreasing tubule diameter.

Consider two adjacent graphene shells, shells  $j$  and  $j+1$  with radii  $R_j$  and  $R_{j+1}$ , in a carbon nanotube, as depicted in Fig. 3. The cylinders can be considered as deformed graphene sheets. Thereby there exist elastic

energies due to bending and radial deformation from the stress free state. Consider three carbon atoms in shell  $j+1$  with separations of  $L$ . For simplicity, we assume that the three atoms lie in the same plane perpendicular to the axis of the tube. Denoting  $R \equiv R_{j+1}$ , the bending energy can be written as

$$\mathcal{E}_\theta = \frac{1}{2}k_\theta L^2 \theta^2 = \frac{1}{2}k_\theta L^2 \left(\frac{L}{R}\right)^2, \quad (1)$$

where  $k_\theta$  is the angular elastic constant between two adjacent bonds. The elastic energy between shells  $j$  and  $j+1$  due to radial deformation is

$$\mathcal{E}_R \cong \frac{1}{2}k_R(R - R_0)^2, \quad (2)$$

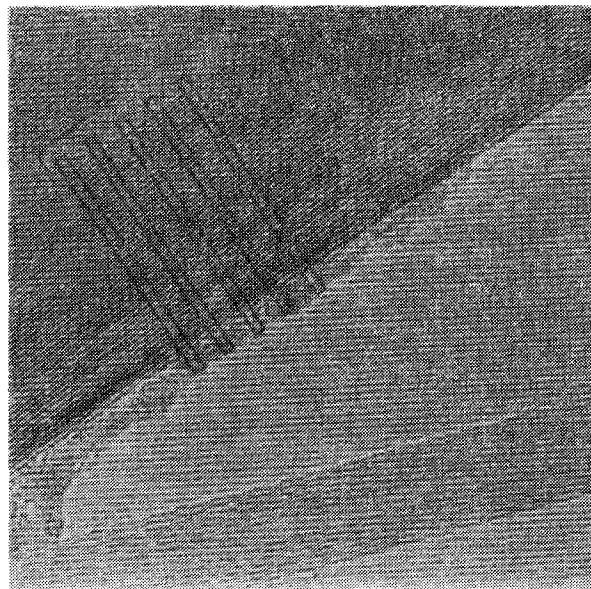


FIG. 1. High resolution transmission electron microscopy images of multi-layer carbon nanotubes. The inter-shell spacing  $\hat{d}_{002}$  was measured in the real space images, as indicated for one of the samples by the boxes in the figure.

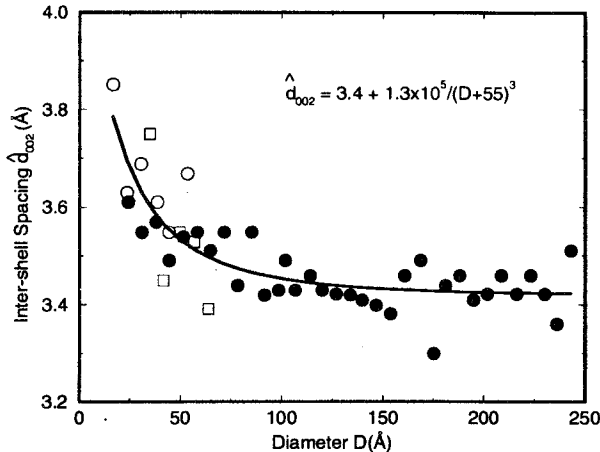


FIG. 2. The least squares fit to the experimental data. The data were measured from three different nanotubes indicated by different symbols. Hollow circles: from a 7-layer tube with innermost diameter  $D_{min} = 17 \text{ \AA}$ ; Solid circles: from a 41-layer tube with  $D_{min} = 26 \text{ \AA}$ ; Hollow squares: from a 6-layer tube with  $D_{min} = 25 \text{ \AA}$ .

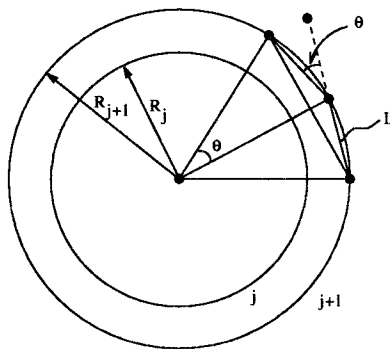


FIG. 3. The force constant model for a carbon nanotube.

where  $k_R$  is the radial elastic constant between the two graphene shells, and  $R_0 = R_j + \Delta$  with  $\Delta$  denoting the equilibrium intershell spacing without any deformation. The equilibrium condition is given by

$$\frac{d\mathcal{E}}{dR} = \frac{d}{dR}(\mathcal{E}_\theta + \mathcal{E}_R) = 0, \quad (3)$$

and therefore we get

$$(R_{j+1} - R_j) \cong \Delta + L \left( \frac{k_\theta}{k_R} \right) \left( \frac{L}{R_{j+1}} \right)^3. \quad (4)$$

This equation is used to perform a least squares fit to the experimental data shown in Fig. 2. The fitting result gives us  $\Delta = 3.4 \text{ \AA}$ , which is the separation of two graphene sheets in graphite, showing consistency of the force constant model. Notice that there is a fitting offset for  $R$ , as shown in Fig. 2. This arises

for two reasons. Firstly, the diameter in the model is not defined in the same way as that in the measurements. Secondly, there may be constraints other than the elastic forces considered in the model (e.g., due to the small number of atoms in the circumferential direction). Also notice that the ratio of elastic constants,  $k_\theta/k_R$ , depends on the value of  $L$ . However, in the case of a carbon nanotube,  $L$  could be quite arbitrary because of the arbitrariness of the chirality for the various tubules.

The simple elastic constant model implies an epitaxy-like growing mechanism for carbon nanotubes. Upon forming the first cylinder of a graphene sheet, the diameter of the second cylinder is determined by the energetic equilibrium between the two graphene shells. This process continues until the curvature of the graphene shells become negligible, so that the elastic energies play less important roles.

The authors are indebted to Dr. S. Iijima for supplying the high resolution TEM image and for valuable discussions. Part of the work by ME is supported by a grant-in-aid for scientific research in priority area "Carbon Cluster" from the Ministry of Education, Science and Culture, Japan. The authors owe sincere thanks to Drs. P.M. Ajayan, G. Dresselhaus and Prof. Patrick Lee for illuminating discussions. The work at MIT is supported by NSF grant DMR-95-10093, and travel support from NSF INT-93-15165 is gratefully acknowledged.

- <sup>1</sup> S. Iijima, Nature **354**, 56 (1991).
- <sup>2</sup> R. Saito, G. Dresselhaus, and M. S. Dresselhaus, J. Appl. Phys. **73**, 494 (1993).
- <sup>3</sup> N. Hamada, S. Sawada, and A. Oshiyama, Phys. Rev. Lett. **68**, 1579 (1992).
- <sup>4</sup> M. R. Pederson and J. Q. Broughton, Phys. Rev. Lett. **69**, 2689 (1992).
- <sup>5</sup> K. Akagi, R. Tamura, and M. Tsukada, Phys. Rev. Lett. **74**, 2307 (1995).
- <sup>6</sup> X. F. Zhang, X. B. Zhang, G. Van Tendeloo, S. Amelinckx, M. Op de Beeck, and J. Van Landuyt, J. Cryst. Growth **130**, 368 (1993).
- <sup>7</sup> T. Yoshikawa and Y. Saito, Phys. Rev. B **48**, 1907 (1993).
- <sup>8</sup> M. Bretz, B. G. Demczyk, and L. Zhang, J. Cryst. Growth **141**, 304 (1994).
- <sup>9</sup> X. Sun, C.-H. Kiang, M. Endo, K. Takeuchi, T. Furuta, and M. S. Dresselhaus, Phys. Rev. B **54**, R12629 (1996).
- <sup>10</sup> T. W. Ebbesen and P. M. Ajayan, Nature **358**, 220 (1992).
- <sup>11</sup> C.-H. Kiang, X. Sun, M. Endo, T. Furuta, S. Iijima, P. M. Ajayan, and M. S. Dresselhaus, in *Fullerenes: Chemistry, Physics and New Directions, Proceedings of the Electrochemical Society*, edited by R. Ruoff and K. Kadish, Electrochemical Society, Los Angeles, CA, 1996.